# Tunable couplers for a modular architecture

August 19, 2024

# 1 Unit cell

## 1.1 Circuit quantization

The unit cell proposed by KIT (Fig. 1) is a fluxonium-like qubit with an integrated readout mode. It uses strips of granular aluminum as compact inductors with high impedances, necessary to reach the fluxonium regime. The circuit has four nodes, however, neglecting parasitic capacitances, one can assume that the central node is not capacitively coupled to any other part of the circuit, and hence it is dynamically frozen. Additionally, the lower node of the circuit is connected to the ground, and therefore its value is zero.

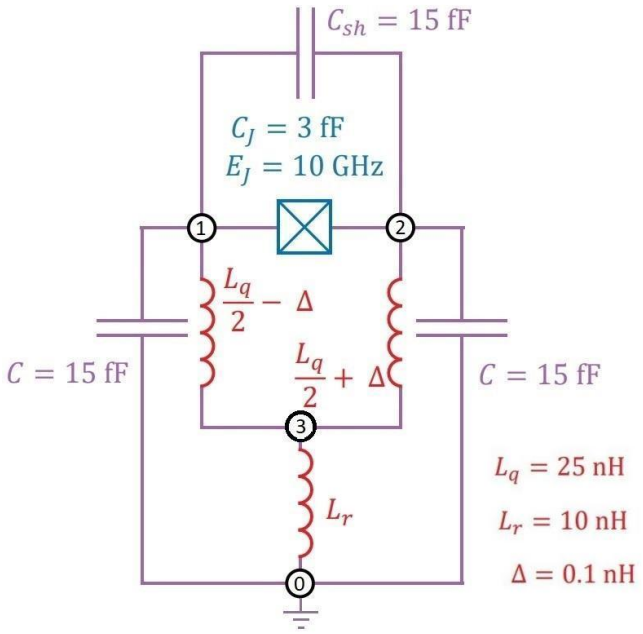


Figure 1: Circuit of the qubit.

The classical Lagrangian of this circuit, in the basis of the node fluxes, $\mathbf{\Phi}_n = \{\Phi_1, \Phi_2, \Phi_3\}$, is:

$$\mathcal{L} = \frac{1}{2}\dot{\mathbf{\Phi}}_n^T \mathbf{C}_n \dot{\mathbf{\Phi}}_n - \frac{1}{2}\mathbf{\Phi}_n^T \mathbf{L}_n^* \mathbf{\Phi}_n + E_J \cos\left[\frac{2\pi}{\Phi_0}\left(\Phi_2 - \Phi_1 + \Phi_{\text{ext}}\right)\right], \tag{1}$$

where $\mathbf{C}_n$ and $\mathbf{L}_n^*$ are the capacitance and inverse inductance matrices of the circuit:

$$\mathbf{C}_n = \begin{bmatrix} C + C_J & -C_J & 0 \\ -C_J & C + C_J & 0 \\ 0 & 0 & 0 \end{bmatrix}, \quad \mathbf{L}_n^* = \begin{bmatrix} L_-^{-1} & 0 & -L_-^{-1} \\ 0 & L_+^{-1} & -L_+^{-1} \\ -L_-^{-1} & -L_+ - ^{-1} & L_-^{-1} + L_+^{-1} + L_r^{-1} \end{bmatrix} \tag{2}$$

To simplify the notation we have called $L_\pm = L_q/2 \pm \Delta$. Also, since the shunting capacitance $C_{\text{sh}}$ and the intrinsic capacitance of the Josephson junction $C_J$ are in parallel, both contribute linearly to the capacitance between nodes 1 and 2, and hence, throughout this document, we will ignore the distinction rename their sum as $C_J \equiv C_J + C_{\text{sh}}$. The presence of a row and column of zeros in the capacitance matrix results from the lack of capacitors connected to the third node of the circuit, and tells us that our basis is not adequate to write the Hamiltonian of the circuit, as this matrix is not invertible. We have to find a basis in which this problem disappears. Applying Kirchoff's law to the third node allows us to find the dependence between the flux at this node and that at the upper nodes:

$$\frac{\Phi_3 - \cancel{\Phi_0}}{L_r} = \frac{\Phi_1 - \Phi_3}{L_-} + \frac{\Phi_2 - \Phi_3}{L_+} \quad \rightarrow \quad \Phi_3 = \gamma\left(L_+\Phi_1 + L_-\Phi_2\right), \tag{3}$$

where

$$\gamma = \frac{4L_r}{l^2}, \quad l^2 = 4\left(L_+L_- + L_+L_r + L_-L_r\right) = L_q(L_q + 4L_r) - 4\Delta^2 \ .$$

With this knowledge, we can define a transformation $\mathbf{P}_1$ to a new set of variables $\mathbf{\Phi}'_n = \{\Phi_1, \Phi_2\}$:

$$\mathbf{\Phi}_n = \mathbf{P}_1\mathbf{\Phi}'_n, \quad \mathbf{P}_1 = \begin{bmatrix} 1 & 0 \\ 0 & 1 \\ \gamma L_+ & \gamma L_- \end{bmatrix} \tag{4}$$

This allows us to rewrite the Lagrangian of the circuit in terms of new capacitance and inverse inductance matrices:

$$\begin{aligned} \mathbf{C}_{n'} &= \mathbf{P}_1^T\mathbf{C}_n\mathbf{P}_1 = \begin{bmatrix} C + C_J & -C_J \\ -C_J & C + C_J \end{bmatrix} \\ \mathbf{L}^*_{n'} &= \mathbf{P}_1^T\mathbf{L}^*_n\mathbf{P}_1 = \begin{bmatrix} L_-^{-1} - \gamma L_+ L_-^{-1} & -\gamma \\ -\gamma & L_+^{-1} - \gamma L_+^{-1} L_- \end{bmatrix} \end{aligned} \tag{5}$$

The next step to obtain the simplest Hamiltonian is to make another change of variables to a basis in which the capacitance matrix is diagonal. We could also diagonalize the inverse capacitance matrix, or we could also diagonalize both (see Appendix **??**), however, this is not that useful because we also want a set of variables in which the Josephson energy can be written in a simple manner. Indeed, looking at the structure of the capacitance matrix $\mathbf{C}'_n$ it is clear that its eigenstates are going to be a symmetric and antisymmetric combination of $\Phi_1$ and $\Phi_2$. Since the Josephson energy depends directly on the difference of these fluxes we can choose our new variables as:

$$\Phi_+ = \Phi_1 + \Phi_2, \quad \Phi_- = \Phi_1 - \Phi_2, \tag{6}$$

The new basis $\mathbf{\Phi}_\pm = \{\Phi_+, \Phi_-\}$ can be obtained by the transformation $\mathbf{P}_2$:

$$\mathbf{\Phi}'_n = \mathbf{P}_2\mathbf{\Phi}_\pm, \quad \mathbf{P}_2 = \frac{1}{2}\begin{bmatrix} 1 & 1 \\ 1 & -1 \end{bmatrix} \tag{7}$$

In this basis, the capacitance matrix is:

$$\mathbf{C}_\pm = \mathbf{P}_2^T\mathbf{C}_{n'}\mathbf{P}_2 = \begin{bmatrix} C/2 & 0 \\ 0 & C/2 + C_J \end{bmatrix} \tag{8}$$

Before transforming the inductance matrix it is useful to rewrite it in terms of a common denominator $l^2$. The off-diagonal terms are easy, since $\gamma = 4L_r/l^2$ already depends on this denominator. The diagonal terms, for example, the first, can be rewritten as:

$$L_-^{-1} - \gamma L_+ L_-^{-1} = \frac{1}{l^2}\left(l^2 L_-^{-1} - 4L_r L_+ L_-^{-1}\right)$$

Noting that

$$l^2 = 4\left(L_+L_- + L_+L_r + L_-L_r\right) \rightarrow l^2L_-^{-1} = 4\left(L_+ + L_r + L_+L_rL_-^{-1}\right) \rightarrow l^2L_-^{-1} - 4L_rL_+L_-^{-1} = 4\left(L_+ + L_r\right)$$

This allows us to write the inverse inductance matrix in a more simplified manner:

$$\mathbf{L}^*_{n'} = \frac{4}{l^2}\begin{bmatrix} L_r + L_+ & -L_r \\ -L_r & L_r + L_- \end{bmatrix} \tag{9}$$

Which now can be easily transformed into our new basis:

$$\mathbf{L}^*_\pm = \mathbf{P}_2^T\mathbf{L}^*_{n'}\mathbf{P}_2 = \frac{1}{l^2}\begin{bmatrix} L_q & 2\Delta \\ 2\Delta & L_q + 4L_r \end{bmatrix} \tag{10}$$

We can now define the charges of the nodes as the canonically conjugate of the momenta of the fluxes

$$Q_+ = \frac{\partial \mathcal{L}}{\partial \Phi_+},\ Q_- = \frac{\partial \mathcal{L}}{\partial \Phi_-},\ \mathbf{Q}_\pm = \{Q_+, Q_-\} \tag{11}$$

Performing a Legendre transformation and elevating the canonical variables to quantum operators finally allows us to obtain the quantum Hamiltonian of the circuit

$$\mathcal{H}(\mathbf{Q}_\pm, \mathbf{\Phi}_\pm) = \mathbf{Q}_\pm^T \mathbf{C}_\pm^{-1} \mathbf{Q}_\pm + \mathbf{\Phi}_\pm^T \mathbf{L}_\pm^* \mathbf{\Phi}_\pm + U_J \tag{12}$$

which can be expanded as:

$$\mathcal{H} = \frac{Q_+^2}{2C_+} + \frac{\Phi_+^2}{2L_+} + \frac{Q_-^2}{2C_-} + \frac{\Phi_-^2}{2L_-} - E_J \cos\left[\frac{2\pi}{\Phi_0}\left(\Phi_- - \Phi_{\text{ext}}\right)\right] + \frac{2\Delta}{l^2}\Phi_+\Phi_- \tag{13}$$

Studying the structure of this Hamiltonian reveals that it can be grouped into three parts. The first one, $\mathcal{H}_+$, contains only elements proportional to the charge and flux operators of the symmetric mode and corresponds to the Hamiltonian of a resonator. The second one, $\mathcal{H}_-$, does the same for the antisymmetric mode and is the Hamiltonian of a fluxonium qubit. The third group, $\mathcal{H}_C$, contains the only element that mixes operators of both modes and represents an inductive coupling between them,

$$\begin{aligned}
\mathcal{H} &= \mathcal{H}_+ + \mathcal{H}_- + \mathcal{H}_C, \\
\mathcal{H}_+ &= \frac{1}{2}\frac{1}{C_+}Q_+^2 + \frac{1}{2}\frac{1}{L_+}\Phi_+^2, \\
\mathcal{H}_- &= \frac{1}{2}\frac{1}{C_-}Q_-^2 + \frac{1}{2}\frac{1}{L_-}\Phi_-^2 - E_J \cos\left[\frac{2\pi}{\Phi_0}\left(\Phi_- - \Phi_{\text{ext}}\right)\right], \\
\mathcal{H}_C &= \frac{1}{L_c}\Phi_+\Phi_-,
\end{aligned} \tag{14}$$

where the effective capacitances of these modes and their coupling are:

$$\begin{aligned}
C_+ = \frac{C}{2}, \quad L_+ = \frac{l^2}{L_q} \approx L_q + 4L_r \\
C_- = \left(\frac{C}{2} + C_J\right), \quad L_- = \frac{l^2}{L_q + 4L_r} \approx L_q, \quad L_C = \frac{l^2}{2\Delta}\ .
\end{aligned}$$

Before we proceed with further analysis of this Hamiltonian it is convenient to consider the range of parameters used in the actual experiments of the circuit, and, consequently, the range of parameters of the resulting effective models.

## 1.2 Analytical limits for the energy levels

The resonator mode can always be solved analytically, and its natural frequency is:

$$\omega_+ = (C_+ L_+)^{-1/2} \tag{15}$$

In some limits the fluxonium can be approximated analytically. This is useful both to obtain insights into the behavior of our unit cell and to know the boundaries in which these limits break. When the fluxonium is threaded by an external flux of $\Phi_{\text{ext}} = \Phi_0/2$ its potential can be written, as a function of the phase across the Josephson junction $\varphi_- = \frac{2\pi}{\Phi_0}\Phi_-$, as:

$$U_- = \frac{E_{L_-}}{2}\varphi_-^2 + E_J \cos(\varphi_-) \tag{16}$$

| | | | | |
|---|---|---|---|---|
| $E_J$ | 1 | - | 15 | GHz |
| $L_r$ | 5 | - | 30 | nH |
| $L_q$ | 10 | - | 50 | nH |
| $\Delta$ | 0 | - | 1 | nH |
| $C$ | 5 | - | 10 | fF |
| $C_J$ | 1 | - | 6 | fF |
| $C_{\text{sh}}$ | 3 | - | 10 | fF |

| | | | | | |
|---|---|---|---|---|---|
| Resonator | $E_{L_+}$ | 1 | - | 5 | GHz |
| | $E_{C_+}$ | 4 | - | 7 | GHz |
| | $\omega_+$ | 5 | - | 18 | GHz |
| Fluxonium | $E_J$ | 1 | - | 15 | GHz |
| | $E_{L_-}$ | 3 | - | 16 | GHz |
| | $E_{C_-}$ | 1 | - | 3 | GHz |
| Coupling | $L_C$ | 150 | - | $\infty$ | nH |

Table 1: Range of parameters of the experimental realization of the circuit (left) and the resulting range of parameters of the effective modes (right). The resonator's natural frequency is $\omega_+ = (L_+C_+)^{-1/2}$.

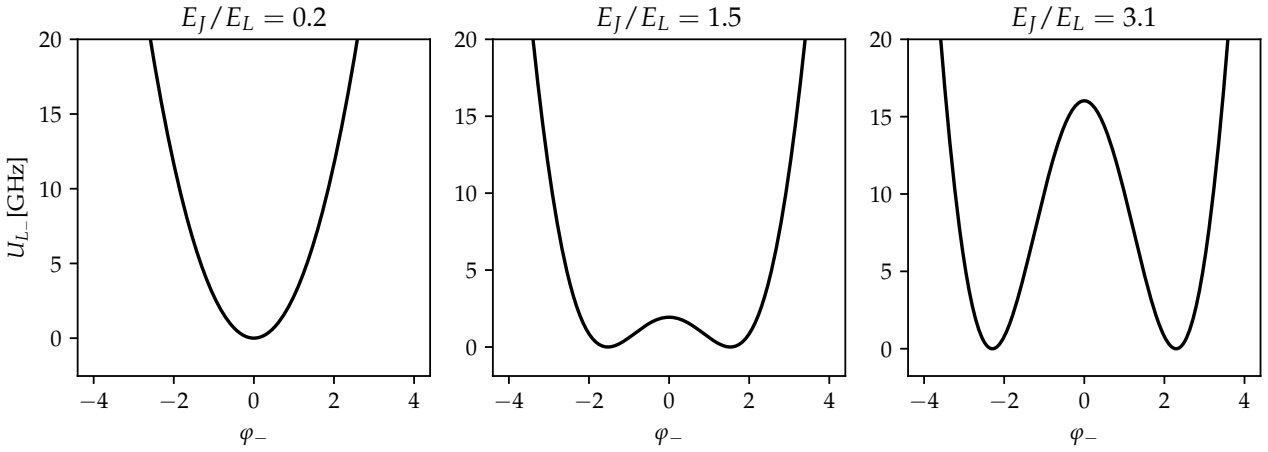


Figure 2: Fluxonium potential at frustration point, eq. (16), for different values of $E_J/E_{L_-}$.

The shape of this potential depends on the ratio between the two energy scales involved and can be in one of three regimes: $E_{L_-} \gg E_J$, $E_{L_-} \approx E_J$, $E_{L_-} \ll E_J$. As shown in Fig. 2 this means that the potential goes from a single-well with some slight perturbations to a double-well potential with a barrier whose height scales as $E_J$. Having a this range of potential shapes allows us to make analytical predictions for the energy levels of the fluxonium, shown in Fig. 3. When $E_J/E_{L-} \ll 1$ the inductive energy dominates and the system will behave more and more as a resonator, meaning that all energy transitions will converge towards the natural frequency of the quadratic part of the fluxonium potential:

$$U_-(E_J \ll E_{L-}) \approx \frac{E_L}{2}\varphi_-^2 \quad \rightarrow \quad \omega_{01} = \omega_{12} = (C_-L_-)^{-1/2} \tag{17}$$

As the Josephson energy increases the system will enter the fluxonium regime, which can't be solved analytically. In this regime, the system transitions from the resonator limit, in which the eigenstates are Hermite polynomials, towards a flux-qubit-like potential, in which the first two eigenstates are a symmetric and antisymmetric combination of Gaussian-like functions centered on the cosine minima. When the Josephson energy is increased further, $E_J/E_{L-} \gg 1$, the cosine potential starts to dominate. This means that the energy barrier inside the harmonic well becomes much larger than the natural frequency of the harmonic well. When this energy barrier is sufficiently large, the eigenstates of the system become isolated within the minima of the cosine potential and interact with the eigenstates of the other minima less and less. In this scenario, the system starts to degenerate and behave as two independent harmonic wells, meaning that the energy levels will be doubly degenerate (one for each of the two minima of the

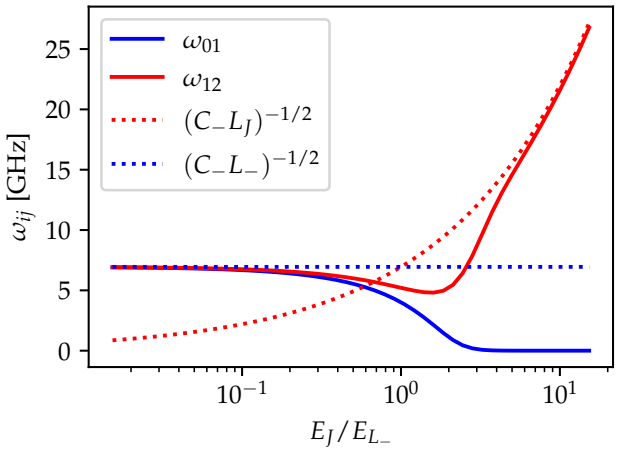


Figure 3: Energy transitions for the fluxonium at the frustration point, eq. (16), for different values of $E_J/E_{L_-}$. The solid lines represent numerical calculations, while the dotted lines correspond to the analytical limits explained in this section.

cosine) and that the energy gaps between them will be approximately given by the harmonic well that best fits the cosine well.

This can be shown with a Talor expansion of the second order of the cosine potential in one of its minima, $\varphi^*$, shown in (18). Indeed, looking at Fig. 3 we can see that the first energy gap calculated numerically becomes zero (showing the degeneracy of the system) and the second energy gap fits the analytical prediction:

$$U_-(E_J \gg E_{L-}) \approx \frac{E_J}{2}\varphi_-^2 \quad \rightarrow \quad L_J = \frac{(\Phi_0/2\pi)^2}{E_J} \quad \rightarrow \quad \omega_{01} \approx 0,\ \omega_{12} \approx (C_- L_J)^{-1/2} \tag{18}$$

## 1.3 Analytical limits for the charge and flux operators

Again, the resonator mode can be solved analytically, and its charge and flux operators can be expressed in the Fock basis as:

$$\begin{aligned} \Phi_+ &= \sqrt{\frac{1}{2}\sqrt{\frac{C_+}{L_+}}}\left(\boldsymbol{a}^\dagger + \boldsymbol{a}\right) = \phi_+\left(\boldsymbol{a}^\dagger + \boldsymbol{a}\right) \\ Q_+ &= i\sqrt{\frac{1}{2}\sqrt{\frac{L_+}{C_+}}}\left(\boldsymbol{a}^\dagger - \boldsymbol{a}\right) = iq_+\left(\boldsymbol{a}^\dagger - \boldsymbol{a}\right) \end{aligned} \tag{19}$$

The charge and flux operators of the fluxonium play a major role in our analysis, and hence, it is convenient to obtain reliable analytical estimations of both. As in the previous section, the factor that will determine their values is the shape of the potential of the fluxonium. When $E_J/E_{L-} \ll 1$, the single-well regime, these operators will be closer and closer to those of the equivalent resonator, eq. (17), and hence the projection of the flux and charge operator on the qubit basis will be:

$$\begin{aligned} P_0\Phi_- P_0 &= \phi_-\boldsymbol{\sigma}^x, \quad \phi_- \approx \sqrt{\frac{1}{2}\sqrt{\frac{L_-}{C_-}}}, \\ P_0 Q_- P_0 &= q_-\boldsymbol{\sigma}^y, \quad q_- \approx \sqrt{\frac{1}{2}\sqrt{\frac{C_-}{L_-}}}, \end{aligned} \tag{20}$$

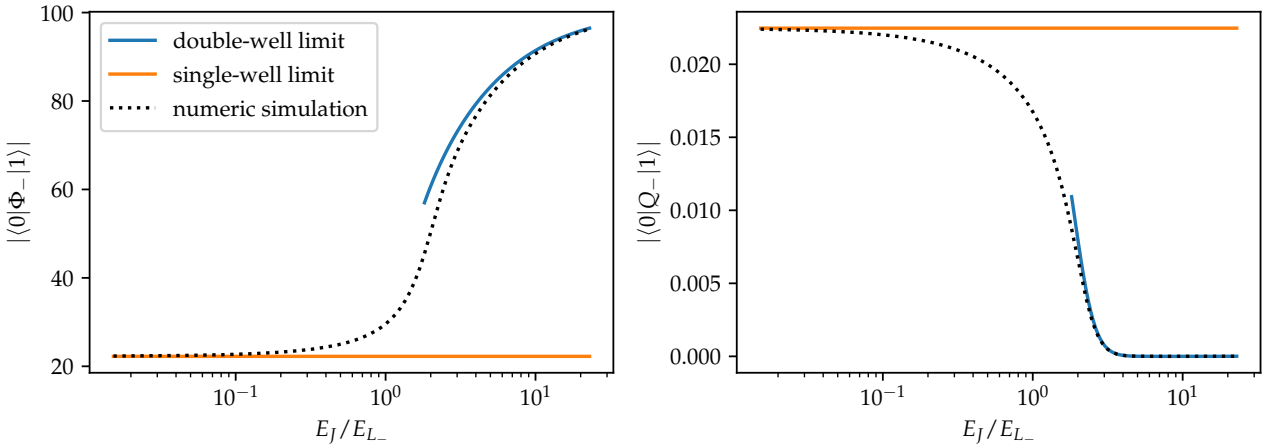


Figure 4: First matrix elements of the flux and charge operators of the fluxonium mode for different values of $E_J$.

In the double-well limit, $E_J/E_{L-} \gg 1$, the wavefunctions ( in the basis of the flux of the fluxonium mode, $\Phi_-$) of the ground and excited states of the fluxonium will be a symmetric and antisymmetric superposition of gaussian-like functions centered on the well's minima. Using symmetry arguments we can write the projection of the flux operator on the qubit basis as

$$P_0\Phi_-P_0 = \langle 0|\Phi_-|1\rangle\,\boldsymbol{\sigma}_x = \phi_-\boldsymbol{\sigma}^x,\ \phi_- \approx \phi_* \tag{21}$$

where $\pm\phi_*$ are the fluxes of the fluxonium's well's minima. In this regime, the charge operator in a fluxonium corresponds to the charge across the Josephson junction, which is the dominant term. The voltage $V_-$ across a Josephson junction is exactly the time derivative of the flux, which in the Heisenberg picture can be written as $V_- = i[H_-, \Phi_-]$. Noting that $Q_- = C_-V_-$ we can approximate analytically the effective charge operator as:

$$P_0Q_-P_0 = P_0iC_-[H_-,\Phi_-]P_0 = iC_-\left[\frac{\omega_-}{2}\boldsymbol{\sigma}^z, \phi_-\boldsymbol{\sigma}^x\right] = iq_-\boldsymbol{\sigma}^y, \quad q_- = C_-\omega_-\phi_- \tag{22}$$

As Fig. 4 shows, indeed, the actual value of theprojections of the charge and flux operators of the fluxonium indeed go from the values predicted by the single-well limit to those of the double-well limit.

## 1.4 Properties of the qubits used in the experiments

The experiment designed by KIT involves three unit cells capacitively coupled, and hence, before analyzing the full system it is convenient to analythe them independently and understand their properties. Table 2 contains the exact values of the experimental parameters for each unit cell.

## 1.5 Analysis of the Internal Coupling

As we are trying to understand this qubit by dividing it into a fluxonium and a resonator, we must have a measure of how much these systems interact. To do so we can express the operators $\Phi_-$ and $\Phi_+$ in the qubit basis (first two eigenstates of the fluxonium) and resonator basis (using Fock states).

We cannot write an equivalent expression for the flux operator of the fluxonium because we don't have an analytical expression of the fluxonium eigenstates, however, we can approximate them. In the fluxonium symmetry point, that is, when an external magnetic flux of half a

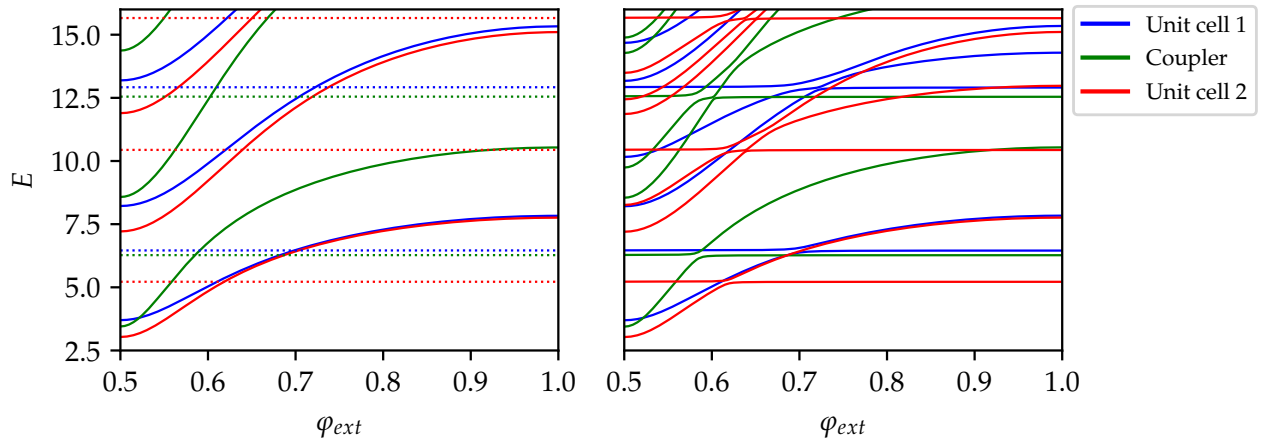


Figure 5: Spectrum of the (left) uncoupled unit cells, that is, $\Delta = 0$, and of the (right) coupled unit cells, $\Delta = 0.5$, used in the experiment.

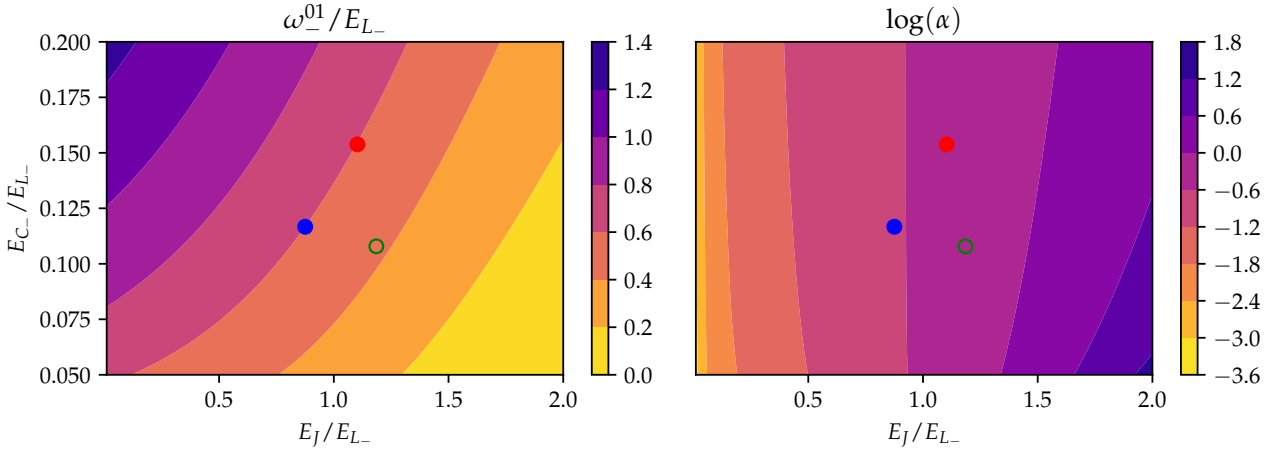


Figure 6: Gap of the unit cell, $\omega_{01}$, for a wide range of experimental parameters. The $y$ axis is the ratio between the capacitive and inductive energy of the fluxonium mode. The $x$ axis is the ratio between the Josephson and inductive energy of the fluxonium mode. The colored dots correspond to the coordinates of the experimental parameters, shown in table 2 for the unit cell 1 (blue), coupler (green) and unit cell 2(red).

| | Unite cell 1 | Coupler | Unit cell 2 |
|---|---|---|---|
| $E_J$ | 5.4 | 9.5 | 5.6 |
| $E_{L_-}$ | 6.2 | 8 | 5.1 |
| $E_{C_-}$ | 0.72 | 0.86 | 0.78 |
| $E_J/E_{L_-}$ | 0.9 | 1.2 | 1.1 |
| $\omega_-$ | 3.70 | 3.45 | 3.03 |
| $\omega_+$ | 6.46 | 6.27 | 5.22 |
| $\alpha$ | 0.22 | 0.48 | 0.37 |

Table 2: Experimental parameters of the unit cells.

magnetic quantum is threaded through the fluxonium loop, its potential becomes a double well (from the cosine term) quadratically confined (from the squared flux term). In this scenario, the ground and excited states of the fluxonium in the phase bases are approximately symmetric and antisymmetric superpositions of Gaussian-like functions centered in the well's minima. Using symmetry arguments we can write the projection of the flux operator on the qubit basis as

$$P_0 \Phi_- P_0 = \langle 0|\Phi_-|1\rangle \, \boldsymbol{\sigma}_x \approx \phi_- \boldsymbol{\sigma}^x, \tag{23}$$

where $\pm\phi_-$ are the fluxes of the fluxonium's well's minima. With this, we can write the projection of the coupling term as:

$$P_0 \frac{\Phi_- \Phi_+}{L_C} P_0 = g_\Phi \, \boldsymbol{\sigma}^x \left(\boldsymbol{a}^\dagger + \boldsymbol{a}\right), \quad g_\Phi = \frac{\phi_- \phi_+}{L_C}\,. \tag{24}$$

Using this analytical approximation yields a coupling strength of $g_{RF}/\omega_{01} \approx 1.5 \times 10^{-2}$, a 1.5% of the qubit's gap, while the numerical calculation using the actual wavefunctions of the fluxonium yields a slightly larger value of $g_{RF}/\omega_{01} \approx 1.9 \times 10^{-2}$.

We have studied how the internal coupling of the circuit created by the asymmetry in the inductances, $\Delta$, changes as it scales. To express the Hamiltonian of the circuit with $\Delta \neq 0$, $H$, in the basis of the circuit with $\Delta = 0$, $P_0$, we employ the Schrieffer-Wolff transformation:

$$H_{\text{eff}} = UPHPU^\dagger = P_0 U H U^\dagger P_0\,, \tag{25}$$

where $U$ is the Schrieffer-Wolff transformation, a rotation that takes operators from the low-energy subspace of a perturbed Hamiltonian to the low-energy subspace of an un-perturbed Hamiltonian:

$$\begin{aligned} UPU^\dagger = P_0 \quad &\rightarrow \quad UP = P_0 U\,, \\ UQU^\dagger = Q_0 \quad &\rightarrow \quad UQ = Q_0 U\,. \end{aligned} \tag{26}$$

The effect of $\Delta$ is twofold. On one hand, as we saw at the end of section 1.1, it introduces an internal coupling between the fluxonium and resonator modes of the circuit $\mathcal{H}_{pert} = 2\Delta \frac{\Phi_- \Phi_+}{l^2}$. On the other hand, it renormalizes the inductances of the resonator and fluxonium modes. As a result, the energies of these modes get modified by a factor that scales as $\Delta^2$.

To ease the analysis, it is also useful to consider the effective Hamiltonian in a first-order perturbation theory, that is, simply the projection of the perturbed Hamiltonian onto the unperturbed basis, $H_{\text{eff}}^{\text{p1}} = P_0 H P_0$. This allows us to understand the internal coupling with parity arguments. Since $\Phi_-$ and $\Phi_+$ are odd operators, the only terms that will survive are those involving interactions between energy levels of the circuit where both the fluxonium and the resonator go from an even state to an odd state or vice-versa. Looking at table **??** and figure 7 we can see that for $\varphi_{\text{ext}} = 0.5$ the first term that will survive is that connecting levels 1 and 3, $\langle 1_{\text{f}}|\Phi_-|0_{\text{f}}\rangle \langle 0_{\text{r}}|\Phi_+|1_{\text{r}}\rangle$, which corresponds to an exchange of a photon between the resonator

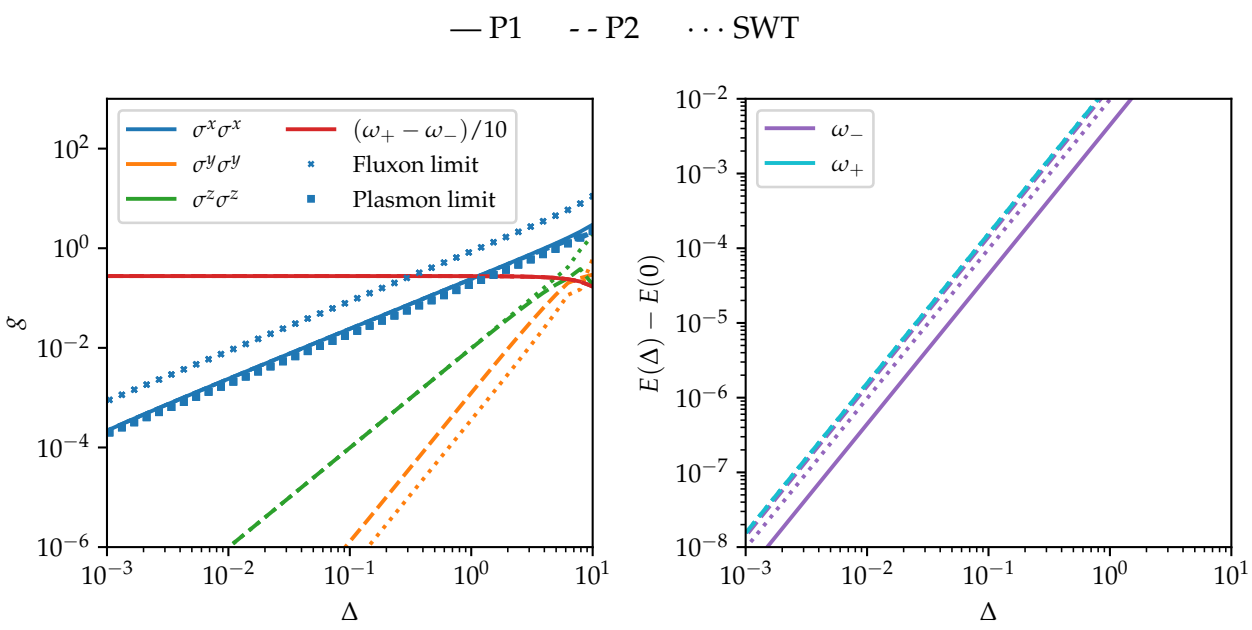


Figure 7: Internal coupling and renormalization of the resonator and fluxonium modes for $\phi_{\text{ext}} = 0.5$.

and fluxonium modes. This can also be understood by writing the interaction in terms of the ladder operators, $\boldsymbol{\sigma}^x = \boldsymbol{\sigma}^+ + \boldsymbol{\sigma}^-$ and applying the rotating wave approximation, which can be a fairly reasonable assumption in certain parameter regimes of the circuit:

$$\boldsymbol{\sigma}^x \left(\boldsymbol{a}^\dagger + \boldsymbol{a}\right) = \left(\boldsymbol{\sigma}^+ + \boldsymbol{\sigma}^-\right)\left(\boldsymbol{a}^\dagger + \boldsymbol{a}\right) = \boldsymbol{\sigma}^+\boldsymbol{a}^\dagger + \boldsymbol{\sigma}^-\boldsymbol{a} \tag{27}$$

This interaction indeed corresponds to the exchange of a photon between the fluxonium and the resonator.

### 1.6 Spectrum and eigenstates

Fig. 8 shows the spectrum of the circuit, the resonator, and the fluxonium as a function of the external magnetic flux. As the figure illustrates, the spectrum of the circuit is well described as an independent fluxonium plus model, excepting the regions of the avoided level crossing.

Fig. 9 contains four subplots labeled (a), (b), (c), and (d). Subplot (a) displays the potential energy and the first two eigenstates of the resonator, and subplot (b) does the same for the fluxonium. Subplots (c) and (d) are the 2D contour plots of the first two eigenstates of the full circuits, where the vertical axis corresponds to $\tilde{\Phi}_+$ and the horizontal axis to $\tilde{\Phi}_-$.

Since subplots (c) and (d) correspond to the tilde variables, the normal modes of the circuit explained in **??**, the wavefunctions are not expressed in the basis corresponding to the resonator and fluxonium modes. This figure shows that the normal modes are only a slight rotation from the fluxonium and resonator modes.

## 2 Effective qubit model

When operated at the frustration point, and considering only the first two levels of the fluxonium—a viable assumption as the model has a large anharmonicity at this regime—the effective spin-boson Hamiltonian of the circuit can be written as:

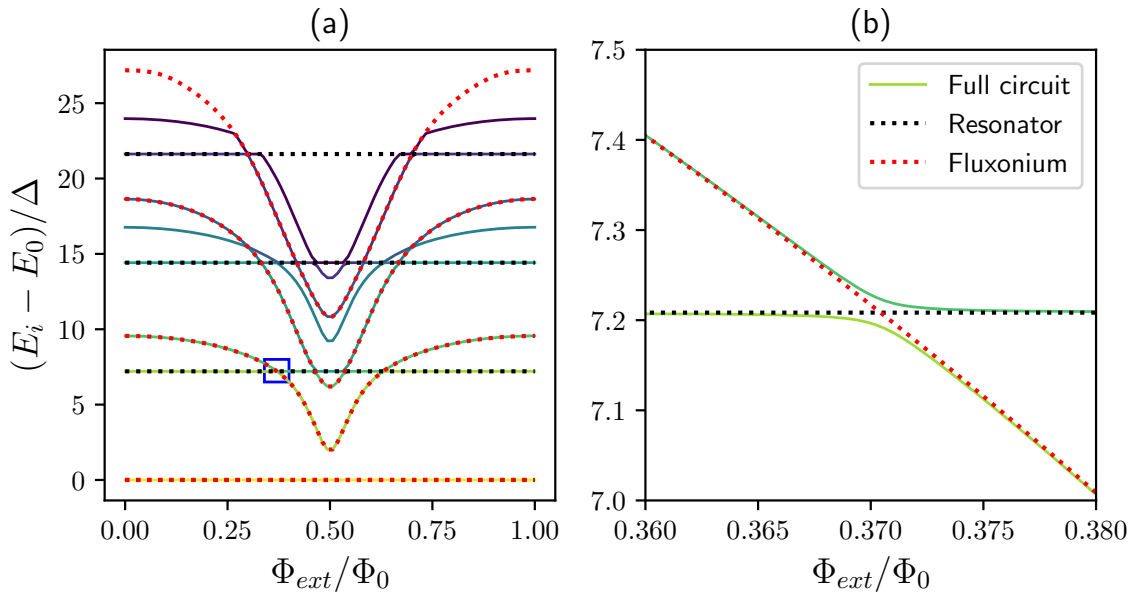


Figure 8: (a) Spectrum of the full circuit, the resonator, and the fluxonium as a function of the external magnetic flux. (b) Zoom to the blue rectangle of the panel (a) highlighting the width of the avoided level crossing.

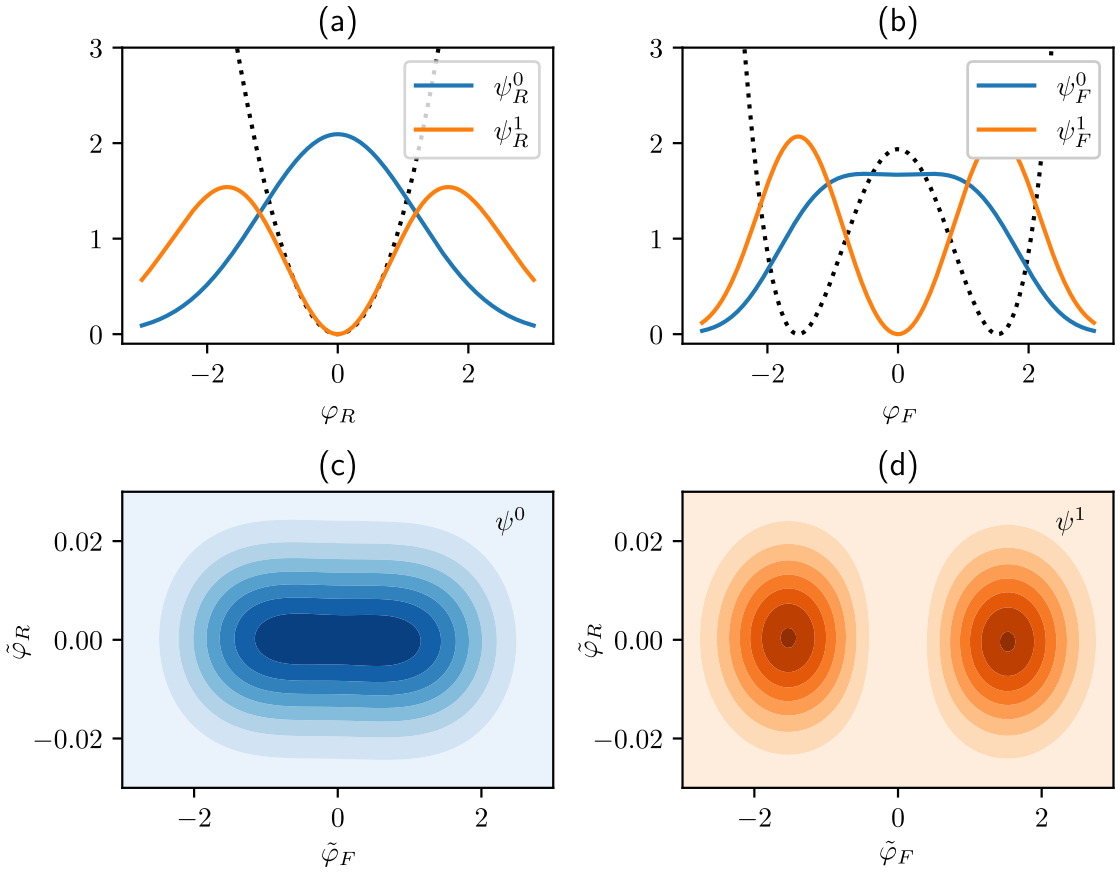


Figure 9: Subplots (a) and (b) show the potential energy and the first two eigenstates of the resonator and the fluxonium, respectively. Subplots (c) and (d) depict the 2D contour plots of the first two eigenstates of the full circuits on the basis of the second transformation, with the vertical axis representing $\tilde{\Phi}_+$ and the horizontal axis representing $\tilde{\Phi}_-$.

$$H = \frac{\omega_-(\varphi_{\text{ext}}^2, \Delta^2)}{2}\boldsymbol{\sigma}^z + \varepsilon(\varphi_{\text{ext}}, \Delta)\boldsymbol{\sigma}^x + g_\Phi(\varphi_{\text{ext}}, \Delta)\boldsymbol{\sigma}^x(\boldsymbol{a}^\dagger + \boldsymbol{a}) + \omega_+(\Delta)\boldsymbol{a}\boldsymbol{a}^\dagger \tag{28}$$

If the difference between the frequencies of the resonator and the fluxonium is considerably smaller than their sum we can apply the RWA. Using ladder operators, $\boldsymbol{\sigma}^x = \boldsymbol{\sigma}^+ + \boldsymbol{\sigma}^-$, $\boldsymbol{\sigma}^y = i(\boldsymbol{\sigma}^- - \boldsymbol{\sigma}^+)$, results in

$$H^q = \frac{\omega_-}{2}\boldsymbol{\sigma}^z + \varepsilon_i(\boldsymbol{\sigma}^+ + \boldsymbol{\sigma}^-) + g_\Phi(\boldsymbol{\sigma}^+\boldsymbol{a}^\dagger + \boldsymbol{\sigma}^-\boldsymbol{a}) + \omega_+\boldsymbol{a}\boldsymbol{a}^\dagger \tag{29}$$

# 3 Two unit cells capacitively coupled

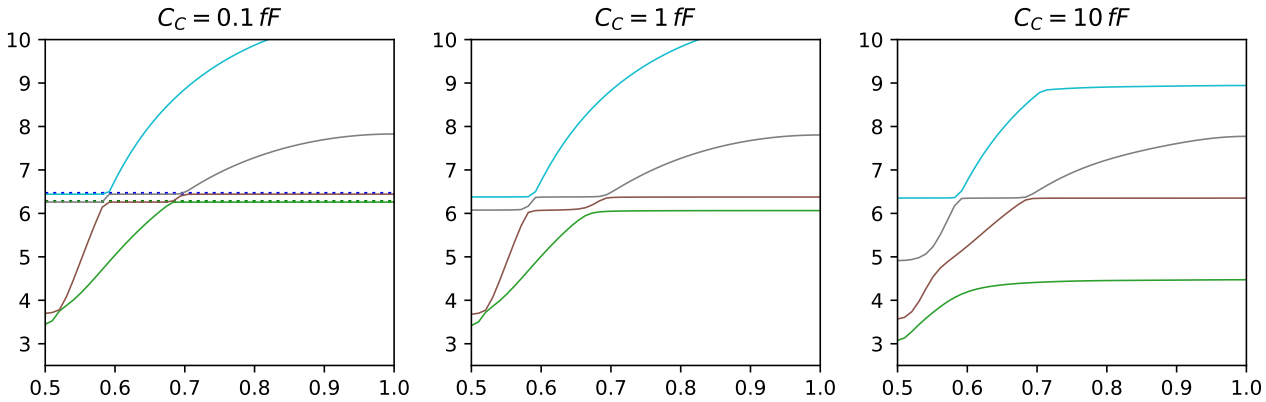


Figure 10: Spectrum of two unit cells capacitively coupled, as a function of the coupling capacitance.

Let's consider only two circuits and couple them with periodic boundary conditions. That is, by coupling the inner nodes together and the outer nodes together, the resulting term in the Lagrangian will be:

$$\mathcal{L}_{\text{int}} = \frac{1}{2}C_C\left(Q_2 - Q_1'\right)^2 + \frac{1}{2}C_C\left(Q_1 - Q_2'\right)^2 \tag{30}$$

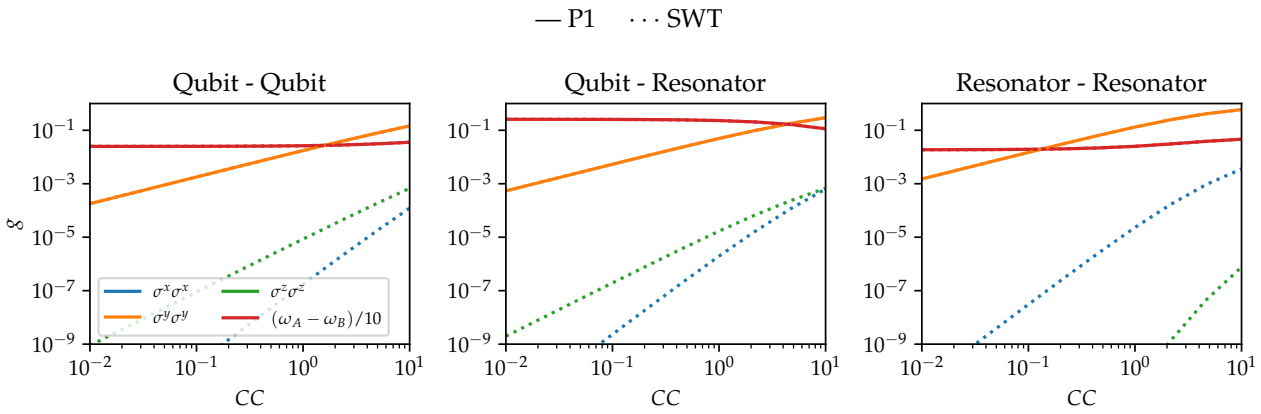


Figure 11: Caption

Where $C_C$ is the value of the coupling capacitance. Performing a change of variables to the resonator and fluxonium modes allows us to write this interaction as:

$$\mathcal{L}_{\text{int}} = \frac{1}{2} C_C \left( \frac{Q_+^2 + Q_-^2 + Q_+'^2 + Q_-'^2}{2} - Q_+ Q_+' + Q_- Q_-' \right) \tag{31}$$

This interaction will modify in the capacitance matrix of the system (in the basis $\{Q_+, Q_-, Q_+', Q_-'\}$). Defining the renormalized capacitances of the modes as $\widetilde{C}_+ = C_+ + C_C/2$ and $\widetilde{C}_- = C_- + C_C/2$ the capacitance matrix will be:

$$\mathbf{C} = \begin{bmatrix} \widetilde{C}_+ & 0 & -C_C/2 & 0 \\ 0 & \widetilde{C}_- & 0 & +C_C/2 \\ -C_C/2 & 0 & \widetilde{C}_+ & 0 \\ 0 & +C_C/2 & 0 & \widetilde{C}_- \end{bmatrix} \tag{32}$$

To obtain the shape of the interaction in the Hamiltonian we have to invert this matrix, which results in:

$$\mathbf{C}^{-1} = \begin{bmatrix} \frac{\widetilde{C}_+}{C_+(C_C+C_+)} & 0 & \frac{C_C}{2C_+(C_C+C_+)} & 0 \\ 0 & \frac{\widetilde{C}_-}{C_-(C_C+C_-)} & 0 & -\frac{C_C}{2C_-(C_C+C_-)} \\ \frac{C_C}{2C_+(C_C+C_+)} & 0 & \frac{\widetilde{C}_+}{C_+(C_C+C_+)} & 0 \\ 0 & -\frac{C_C}{2C_-(C_C+C_-)} & 0 & \frac{\widetilde{C}_-}{C_-(C_C+C_-)} \end{bmatrix} \tag{33}$$

which in the limit $C_C/C \ll 1$ can be approximated up to the first order as:

$$\mathbf{C}^{-1} \approx \begin{bmatrix} \frac{1}{\widetilde{C}_+} & 0 & \frac{C_C/2}{C_+^2} & 0 \\ 0 & \frac{1}{\widetilde{C}_-} & 0 & -\frac{C_C/2}{C_-^2} \\ \frac{C_C/2}{C_+^2} & 0 & \frac{1}{\widetilde{C}_+} & 0 \\ 0 & -\frac{C_C/2}{C_-^2} & 0 & \frac{1}{\widetilde{C}_-} \end{bmatrix} \tag{34}$$

The effects described by this matrix are twofold. First, a renormalization of the resonator and the fluxonium modes. Second, a capacitive resonator-resonator and fluxonium-fluxonium interaction.

The Hamiltonian of the circuit would be the sum of the individual Hamiltonians of the qubits plus a capacitive interaction between their resonator and fluxonium modes. Note that as a result of using periodic boundary conditions, that is, by also coupling the outer nodes of the circuits we have effectively eliminated the crossed coupling between the fluxonium of one qubit and the resonator of the other qubit, and vice versa.

# 4 Three unit cells capacitively coupled

## 4.1 Effective low-energy model

$$H = H_1 + H_c + H_2 + H_{q_{1c}} + H_{q_{c2}} + H_{q_{12}} \tag{35}$$

$$\begin{aligned}
H_1 &= \frac{\omega_{1-}}{2}\boldsymbol{\sigma}^z + \mu_1\boldsymbol{\sigma}^x + \omega_{1+}\boldsymbol{a}\boldsymbol{a}^\dagger + g_{\Phi_1}\boldsymbol{\sigma}^x(\boldsymbol{a}^\dagger + \boldsymbol{a}) + ig_{q_1}\boldsymbol{\sigma}^y(\boldsymbol{a}^\dagger - \boldsymbol{a}) \\
H_c &= \frac{\omega_{c-}}{2}\boldsymbol{\sigma}^z + \mu_c\boldsymbol{\sigma}^x + \omega_{c+}\boldsymbol{a}\boldsymbol{a}^\dagger + g_{\Phi_c}\boldsymbol{\sigma}^x(\boldsymbol{a}^\dagger + \boldsymbol{a}) \\
H_2 &= \frac{\omega_{2-}}{2}\boldsymbol{\sigma}^z + \mu_2\boldsymbol{\sigma}^x + \omega_{2+}\boldsymbol{a}\boldsymbol{a}^\dagger + g_{\Phi_2}\boldsymbol{\sigma}^x(\boldsymbol{a}^\dagger + \boldsymbol{a}) + ig_{q_2}\boldsymbol{\sigma}^y(\boldsymbol{a}^\dagger - \boldsymbol{a}) \\
H_{q_{1c}} &= g_{q_{1c}}\boldsymbol{\sigma}^y\boldsymbol{\sigma}^y \\
H_{q_{c2}} &= g_{q_{c2}}\boldsymbol{\sigma}^y\boldsymbol{\sigma}^y \\
H_{q_{12}} &= g_{q_{12}}\boldsymbol{\sigma}^y\boldsymbol{\sigma}^y
\end{aligned} \tag{36}$$

$$\begin{aligned}
\mu_1 &= -E_{J_1}\langle 0|\sin(\varphi_{1-} - 0.5)|1\rangle(\varphi_{\text{ext}} - 0.5) \\
\mu_c &= -E_{J_c}\langle 0|\sin(\varphi_{c-} - 0.5)|1\rangle(\varphi_{\text{ext}} - 0.5) \\
\mu_2 &= -E_{J_2}\langle 0|\sin(\varphi_{2-} - 0.5)|1\rangle(\varphi_{\text{ext}} - 0.5)
\end{aligned} \tag{37}$$

$$\begin{aligned}
g_{\Phi_i} &= \frac{1}{L_{2_i}}\langle 0|\Phi_{i+}|1\rangle\langle 0|\Phi_{i-}|1\rangle \\
g_{q_i} &= \frac{1}{2_{2_i}}\langle 0|Q_{i+}|1\rangle\langle 0|Q_{i-}|1\rangle
\end{aligned} \tag{38}$$

$$\begin{aligned}
g_{q_{1c}} &= \frac{1}{C_{C_{1c}}}\langle 0|Q_{1-}|1\rangle\langle 0|Q_{c-}|1\rangle \\
g_{q_{c2}} &= \frac{1}{C_{C_{c2}}}\langle 0|Q_{c-}|1\rangle\langle 0|Q_{2-}|1\rangle \\
g_{q_{12}} &= \frac{1}{C_{C_{12}}}\langle 0|Q_{1-}|1\rangle\langle 0|Q_{2-}|1\rangle
\end{aligned} \tag{39}$$

### 4.1.1 Effective two-body model

To obtain the effective Hamiltonian in which the degrees of freedom of the coupler qubit are traced out we can first assume that the coupling between the qubit and resonator modes can be neglected when out of resonance, and hence the problem can be decoupled in two parts. First, the part containing the qubit terms:

$$\begin{aligned}
H = &\sum_{i=1,c,2}\omega_{i-}\boldsymbol{b}_i\boldsymbol{b}_i^\dagger + \mu_i(\boldsymbol{b}_i^\dagger + \boldsymbol{b}_i) \\
&-\sum_{i=1,2}g_{q_{ic}}(\boldsymbol{b}_i^\dagger - \boldsymbol{b}_i)(\boldsymbol{b}_c^\dagger - \boldsymbol{b}_c) \\
&-g_{q_{12}}(\boldsymbol{b}_1^\dagger - \boldsymbol{b}_1)(\boldsymbol{b}_2^\dagger - \boldsymbol{b}_2)
\end{aligned} \tag{40}$$

expanding the parenthesis:

$$\begin{aligned}
H = &\sum_{i=1,c,2}\omega_{i-}\boldsymbol{b}_i\boldsymbol{b}_i^\dagger + \mu_i(\boldsymbol{b}_i^\dagger + \boldsymbol{b}_i) \\
&-\sum_{i=1,2}g_{q_{ic}}(\boldsymbol{b}_i^\dagger\boldsymbol{b}_c^\dagger + \boldsymbol{b}_i\boldsymbol{b}_c - \boldsymbol{b}_i^\dagger\boldsymbol{b}_c - \boldsymbol{b}_i\boldsymbol{b}_c^\dagger) \\
&-g_{q_{12}}(\boldsymbol{b}_1^\dagger\boldsymbol{b}_2^\dagger + \boldsymbol{b}_1\boldsymbol{b}_2 - \boldsymbol{b}_1^\dagger\boldsymbol{b}_2 - \boldsymbol{b}_1\boldsymbol{b}_2^\dagger)
\end{aligned} \tag{41}$$

## 4.2 Effective coupling between qubits 1 and 3

The following section develops the theory to obtain the effective coupling between qubits 1 and 3, mediated by qubit 2.

The Lagrangian of three unit cells with nearest neighbor capacitive coupling and open boundary conditions is:

$$\mathcal{L} = \mathcal{L}_0 + \frac{1}{2}C_C\left((\dot{\Phi}_{2,1} - \dot{\Phi}_{1,2})^2 + (\dot{\Phi}_{2,2} - \dot{\Phi}_{1,3})^2\right) \tag{42}$$

where $\mathcal{L}_\prime$ is the Lagrangian of the uncoupled system, $C_C$ is the capacitance of the coupling between adjacent unit cells and $\Phi_{j,i}$ is the flux at node $j$ of unit cell $i$. This interaction can be rewritten in terms of the resonator (+) and qubit (−) variables of each unit cell, $\Phi_{\pm,i} = \Phi_{1,i} \pm \Phi_{2,i}$, which in matrix form can be written as:

$$\mathcal{L} = \mathcal{L}_0 + \frac{1}{2}\dot{\mathbf{\Phi}}_\pm^T \mathbf{C}_{\text{int}} \dot{\mathbf{\Phi}}_\pm \tag{43}$$

Here, $\dot{\mathbf{\Phi}}_\pm = \{\Phi_{-,1}, \Phi_{+,1}, \Phi_{-,2}, \Phi_{+,2}, \Phi_{-,3}, \Phi_{+,3}\}$, and

$$\mathbf{C}_{\text{int}} = C_C \begin{bmatrix} 1/4 & -1/4 & 1/4 & 1/4 & 0 & 0 \\ -1/4 & 1/4 & -1/4 & -1/4 & 0 & 0 \\ 1/4 & -1/4 & 1/2 & 0 & 1/4 & 1/4 \\ 1/4 & -1/4 & 0 & 1/2 & -1/4 & -1/4 \\ 0 & 0 & 1/4 & -1/4 & 1/4 & 1/4 \\ 0 & 0 & 1/4 & -1/4 & 1/4 & 1/4 \end{bmatrix} \tag{44}$$

This capacitive matrix includes two types of terms. The elements in the diagonal will add to those of the capacitance matrix of the uncoupled system and will renormalize the capacitances of the qubit and resonator modes. The capacitances of the off-diagonal will result in capacitive couplings between the resonator and qubit modes of each unit cell in the Hamiltonian, resulting from the inversion of this matrix.

This Hamiltonian is rather complex, as it includes capacitive interactions between all its modes. Nevertheless, since we are going to study the effective coupling between qubits 1 and 3, mediated by qubit 2, when all of the qubits are off-resonance from their resonators, the first approximation that we can make to simplify the problem is to neglect the effect of the resonators in the experiment. Under this simplification, the Hamiltonian of three qubits capacitively coupled can be written as:

$$H = \sum_i H_{0,i} + \frac{1}{C_{12}}Q_1Q_2 + \frac{1}{C_{23}}Q_2Q_3 + \frac{1}{C_{13}}Q_1Q_3 \tag{45}$$

Where $H_{0,i}$ is the Hamiltonian of the uncoupled qubit $i$. The effective coupling between qubits 1 and 3 can be calculated by defining a low-energy subspace, $\{|000\rangle, |100\rangle, |001\rangle, |101\rangle\}$, and then using the Schrieffer-Wolff transformation (SWT) [1] to obtain the coupling between the states $|100\rangle, |001\rangle$ when written in the basis of the eigenstates of the low-energy subspace of the uncoupled qubits. The SWT can be calculated numerically and without approximation as explained in ref. [2], but it can also be calculated analytically using perturbation theory. Figure 12 the mediated coupling obtained thorugh (i) experiment, (ii) second-order SWT calculated semi-analytically and (iii) full SWT calculated numerically

The first step to approach this problem analytically is to project Hamiltonian (45) onto the energy subspace of up to one excitation in each qubit, $\{|0\rangle, |1\rangle\}_0 \otimes \{|0\rangle, |1\rangle\}_1 \otimes \{|0\rangle, |1\rangle\}_2$. On this low-energy basis, the Hamiltonian can be written as:

$$H_{\text{low}} = \frac{\omega_1}{2}\boldsymbol{\sigma}_1^z + \frac{\omega_2}{2}\boldsymbol{\sigma}_2^z + \frac{\omega_3}{2}\boldsymbol{\sigma}_3^z + g_{12}\boldsymbol{\sigma}_1^y\boldsymbol{\sigma}_2^y + g_{23}\boldsymbol{\sigma}_2^y\boldsymbol{\sigma}_3^y + g_{13}\boldsymbol{\sigma}_1^y\boldsymbol{\sigma}_3^y \tag{46}$$

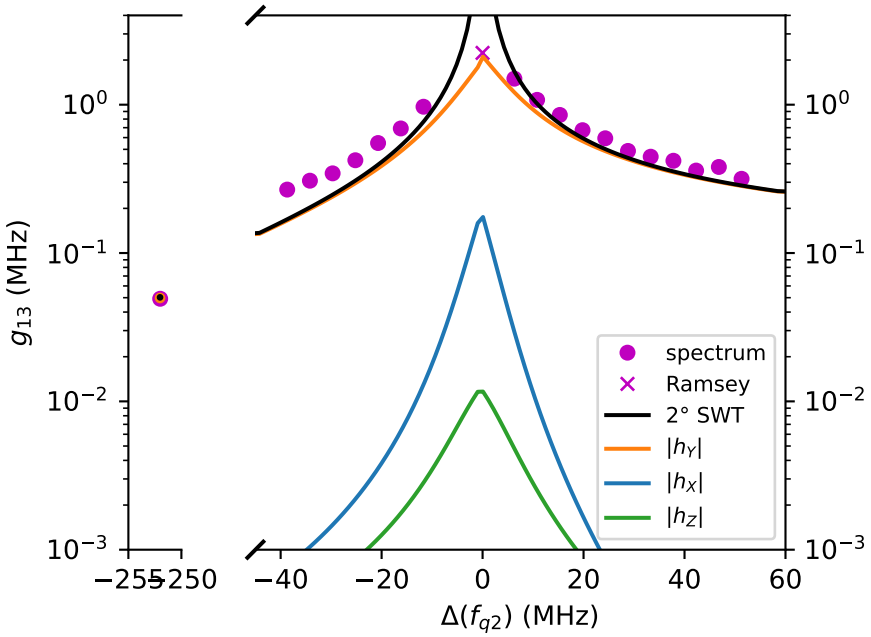


Figure 12: Effective mediated coupling between qubits 1 and 3, when these are on resonance, as a function of the detuning of qubit 2. The different lines correspond to the effective coupling obtained experimentally (magenta) through spectrometry (dots) and Ramsay interferometry (cross), through the second-order SWT obtained semi-analitically (black) and through the full SWT obtained numerically (orange, blue, green). The black line corresponding to the second order represents the coefficient of the coupling proportional to $\boldsymbol{\sigma}_1^y \boldsymbol{\sigma}_3^y$, whereas the lines for the full SWT also includes contributions proportional to $\boldsymbol{\sigma}_1^x \boldsymbol{\sigma}_3^x$ and $\boldsymbol{\sigma}_1^z \boldsymbol{\sigma}_3^z$.

Here $g_{ij} = \frac{1}{C_{ij}} \langle 0_i|Q_i|1_i\rangle \langle 0_j|Q_j|1_j\rangle$ and $C_{ij}$ is the relevant term obtained from the inverse of the capacitance matrix.

We are now ready to use the SWT to calculate perturbatively the effective version of this Hamiltonian in the low-energy subspace $\{|000\rangle, |100\rangle, |001\rangle, |101\rangle\}$. The first step to do so is to divide our low energy Hamiltonian into an unperturbed Hamiltonian, $H_0 = \frac{\omega_1}{2}\boldsymbol{\sigma}_1^z + \frac{\omega_2}{2}\boldsymbol{\sigma}_2^z + \frac{\omega_3}{2}\boldsymbol{\sigma}_3^z$, plus a perturbation, $V = g_{12}\boldsymbol{\sigma}_1^y\boldsymbol{\sigma}_2^y + g_{23}\boldsymbol{\sigma}_2^y\boldsymbol{\sigma}_3^y + g_{13}\boldsymbol{\sigma}_1^y\boldsymbol{\sigma}_3^y$.

The first-order expansion of the effective Hamiltonian is then $H_{\text{eff},1} = H_0 + P_0 V P_0$, where $P0$ is the projector onto the eigenstates of the low-energy unperturbed Hamiltonian $H_0$. Since the operator $\boldsymbol{\sigma}^y$ flips the state of the qubit, the only coupling term that survives in this first-order expansion is the direct coupling between qubits 1 and 3, that is:

$$\langle 100|H_{\text{eff},1}|001\rangle = \langle 100|V|001\rangle = \langle 100|g_{13}\boldsymbol{\sigma}_1^y\boldsymbol{\sigma}_3^y|001\rangle = -g_{13}\langle 100|100\rangle = -g_{13} \tag{47}$$

It can be easily shown that the rest of the relevant matrix elements will be $\langle 001|H_{\text{eff},1}|100\rangle = -\langle 000|H_{\text{eff},1}|101\rangle = -\langle 101|H_{\text{eff},1}|000\rangle$, and hence, the first order expansion can be written as:

$$H_{\text{eff},1} = \frac{\omega_1}{2}\boldsymbol{\sigma}_1^z + \frac{\omega_3}{2}\boldsymbol{\sigma}_3^z + g_{13}\boldsymbol{\sigma}_1^y\boldsymbol{\sigma}_3^y \tag{48}$$

The second-order expansion of the effective Hamiltonian includes interactions mediated by energy states not included in our subspace of interest:

$$H_{\text{eff},2} = H_0 + P_0 V P_0 + \frac{1}{2}\sum_{ijk}\left(\frac{1}{E_i - E_k} + \frac{1}{E_j - E_k}\right)\langle i|V|k\rangle\langle k|V|j\rangle\,|i\rangle\langle j|\ , \tag{49}$$

where in the summation the indices $i$ and $j$ correspond to the states included in our subspace and the index $k$ the mediating states. The first obvious candidate to mediate this interaction

is the state with one excitation on the middle qubit. The contribution through this state is:

$$\frac{1}{2}\left(\frac{1}{E_{100}-E_{010}}+\frac{1}{E_{001}-E_{010}}\right)\langle 100|V|010\rangle\langle 010|V|001\rangle \tag{50}$$

Since this is the case in the experiment we are going to consider that qubits 1 and 3 are on resonance, that is, $\omega_1=\omega_3=\omega$. Defining $\Delta=\omega_1-\omega_2$ and $\Sigma=\omega_1+\omega_2$, the previous equation can be written as:

$$\frac{g_{12}g_{23}}{\Delta} \tag{51}$$

The next state that will contribute as a mediator of interactions is the state of one excitation on each qubit. The contribution of this state to the interaction between the qubits at the extreme will be:

$$\frac{1}{2}\left(\frac{1}{E_{100}-E_{111}}+\frac{1}{E_{001}-E_{111}}\right)\langle 100|V|111\rangle\langle 111|V|001\rangle=-\frac{g_{12}g_{23}}{\Sigma} \tag{52}$$

The rest of the mediating states will result in either a null contribution by parity arguments or will result in a lower contribution because of the larger energy differences.

Extending this analysis to the rest of the elements of the effective Hamiltonian allows us to conclude that the second-order expansion is:

$$H_{\text{eff},2}=\frac{\tilde{\omega}}{2}(\boldsymbol{\sigma}_1^z+\boldsymbol{\sigma}_3^z)+\tilde{g}\boldsymbol{\sigma}_1^y\boldsymbol{\sigma}_3^y\ , \tag{53}$$

where

$$\tilde{\omega}=\omega+g_{12}g_{23}\left(\frac{1}{\Delta}-\frac{1}{\Sigma}\right) \tag{54}$$

and

$$\tilde{g}=g_{12}g_{23}\left(\frac{1}{\Delta}-\frac{1}{\Sigma}\right)+g_{13} \tag{55}$$

The last question of interest that remains is to consider the value of the coupling at maximum detuning. In this scenario, the initial approximation to assume that the effect of the resonators could be neglected is no longer valid, as the detuning between the resonators will be of the same order of magnitude as the detuning of qubit 2. Including the resonators in the Hamiltonian will not affect the first-order expansion of the effective Hamiltonian, as only direct interactions appear there. However, since the second resonator (subindex 2r) is directly coupled to both qubits 1 and 3 it can mediate an interaction. Hence, the relevant contributions to the effective Hamiltonian will be through state with one photon in the second resonator $|000100\rangle$, and the state with one photon qubit 1, resonator 2 and qubit 3, $|100110\rangle$:

$$\frac{1}{2}\left(\frac{1}{E_{100000}-E_{000100}}+\frac{1}{E_{000001}-E_{000100}}\right)\langle 100000|V|000100\rangle\langle 000100|V|000001\rangle=\frac{g_{1,2r}g_{2r,3}}{\omega-\omega_{+,2}} \tag{56}$$

and

$$\frac{1}{2}\left(\frac{1}{E_{100000}-E_{100110}}+\frac{1}{E_{000001}-E_{100110}}\right)\langle 100000|V|100110\rangle\langle 100110|V|000001\rangle=-\frac{g_{1,2r}g_{2r,3}}{\omega+\omega_{+,2}} \tag{57}$$

where

$$g_{1,2r}=\frac{1}{C_{1,2r}}\langle 0_1|Q_1|1_1\rangle\langle 0_2r|Q_2r|1_2r\rangle=\frac{1}{C_{1,2r}}\langle 0_1|Q_1|1_1\rangle\sqrt{\frac{1}{2}\sqrt{\frac{L_{2r}}{C_{2r}}}}$$

$$g_{2r,3}=\frac{1}{C_{2r,3}}\langle 0_3|Q_3|1_3\rangle\langle 0_2r|Q_2r|1_2r\rangle=\frac{1}{C_{2r,3}}\langle 0_3|Q_3|1_3\rangle\sqrt{\frac{1}{2}\sqrt{\frac{L_{2r}}{C_{2r}}}}$$

and $C_{1,2r}$ and $C_{2r,3}$ are the matrix elements of the inverse capacitance matrix between qubit 1 and resonator 2, and resonator 2 and qubit 3, respectively.

This last result allows us to conclude that the effective coupling between qubits 1 and 3 when qubit 2 is very detuned from them, that is, the static coupling, is:

$$\tilde{g}(\Delta \gg 1) = g_{13} + g_{1,2r} g_{2r,3} \left( \frac{1}{\omega - \omega_{+,2}} - \frac{1}{\omega + \omega_{+,2}} \right) \tag{58}$$

# 5 Chain of capacitively coupled qubits

A chain of capacitively coupled qubits would include the Hamiltonian of the individual qubits plus a capacitive coupling that depends on the square of the charge difference of the nodes involved in the coupling. Written in terms of the node operators, the coupling term would appear in the Lagrangian of the chain as:

$$\mathcal{L}_C = \sum_{i=0}^{N-1} \frac{C_C}{2} \left(Q_2^{i+1} - Q_1^i\right)^2 \tag{59}$$

Substituting the node charges for the fluxonium and resonator charges, $Q_1 = (Q_+ + Q_-)/2$ and $Q_2 = (Q_+ - Q_-)/2$, results in:

$$\mathcal{L}_C = \sum_{i=0}^{N-1} \frac{C_C}{4} \left({Q_+^i}^2 + {Q_-^i}^2 - Q_+^i Q_+^{i+1} + Q_-^i Q_-^{i+1} - Q_+^i Q_-^{i+1} + Q_-^i Q_+^{i+1}\right), \tag{60}$$

To obtain the Hamiltonian of the chain we have to write and invert the capacitive matrix of the system, now corresponding to the charge variables $\left\{Q_+^0, Q_-^0, \ldots, Q_+^N, Q_-^N\right\}$. The analytical inverse of this matrix for a generic chain of N spins is a cumbersome result, and hence, to study the general properties of the system it is convenient to calculate the inverse of the matrix as an approximate series in powers of $\varepsilon = (C_C/2)/C \ll 1$. Under this change of variables the capacitance matrix can be written as:

$$\frac{\mathbf{C}}{C} = \hat{\mathbf{C}} = \begin{bmatrix} \widetilde{C}_+/C & 0 & -\varepsilon & +\varepsilon & 0 & 0 & \\ 0 & \widetilde{C}_-/C & -\varepsilon & +\varepsilon & 0 & 0 & \\ -\varepsilon & +\varepsilon & \widetilde{C}_+/C & 0 & -\varepsilon & +\varepsilon & \\ -\varepsilon & +\varepsilon & 0 & \widetilde{C}_-/C & -\varepsilon & +\varepsilon & \ddots \\ 0 & 0 & -\varepsilon & +\varepsilon & \widetilde{C}_+/C & 0 & \\ 0 & 0 & -\varepsilon & +\varepsilon & 0 & \widetilde{C}_-/C & \\ & & \ddots & & & & \end{bmatrix} \tag{61}$$

The inverse of this matrix can be approximated by decomposing it in a diagonal $\mathbf{D}$ and an off-diagonal $\mathbf{R}$ matrix, and expanding this in a Taylor series:

$$\hat{\mathbf{C}}^{-1} = \frac{1}{\mathbf{D} + \varepsilon\mathbf{R}} \approx \left(\frac{1}{\mathbf{D}} - \varepsilon\frac{\mathbf{R}}{\mathbf{D}^2}\right) + O(\varepsilon^2) \tag{62}$$

Keeping only the first order in $\varepsilon$ gives us a quite simple expression for the inverse, which can be written as:

$$\mathbf{C}^{-1} \approx \frac{1}{C} \begin{bmatrix} 1-\varepsilon & 0 & \varepsilon & \varepsilon & 0 & 0 & \\ 0 & 1-\varepsilon & \varepsilon & \varepsilon & 0 & 0 & \\ \varepsilon & \varepsilon & 1-\varepsilon & 0 & \varepsilon & \varepsilon & \\ \varepsilon & \varepsilon & 0 & 1-\varepsilon & -\varepsilon & \varepsilon & \ddots \\ 0 & 0 & \varepsilon & \varepsilon & 1-\varepsilon & 0 & \\ 0 & 0 & \varepsilon & \varepsilon & 0 & 1-\varepsilon & \\ & & \ddots & & & & \end{bmatrix} \tag{63}$$

Keeping higher orders of the expansion would result in couplings with the n-th neighboring cells proportional to $\varepsilon^n$. With this approximation, we can decompose the Hamiltonian of a chain of capacitively coupled qubits as:

$$H = \sum_{i=0}^{N} \left(H_i^q + H_i^c\right) \tag{64}$$

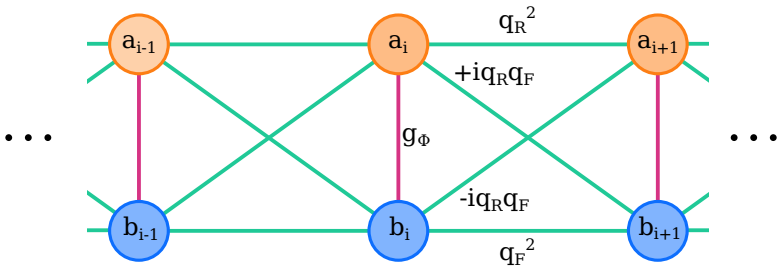


Figure 13: Caption

The Hamiltonian of each qubit will be renormalized by the capacitive term. The unit cell term is:

$$H_i^q = \frac{\omega_-}{2}\boldsymbol{\sigma}_i^z + \omega_+ \boldsymbol{a}_i \boldsymbol{a}_i^\dagger + g_\Phi \boldsymbol{\sigma}_i^x (\boldsymbol{a}_i^\dagger + \boldsymbol{a}_i) \tag{65}$$

The coupling term can be written as:

$$H_i^c = \frac{C_C}{2C^2}\left(Q_-^i Q_-^{i+1} + Q_+^i Q_+^{i+1} + Q_-^i Q_+^{i+1} + Q_+^i Q_-^{i+1}\right) \tag{66}$$

Projecting the charge operators of the fluxonium in the qubit basis and writing the charge operators of the resonator in the fock basis results in:

$$\begin{aligned} H_i^c = -\frac{C_C}{C^2}\Bigg[&(C_-\omega_-\phi_*)^2 \boldsymbol{\sigma}_i^y \boldsymbol{\sigma}_{i+1}^y + \frac{1}{2}\sqrt{\frac{L_+}{C_+}}(\boldsymbol{a}_i^\dagger - \boldsymbol{a}_i)(\boldsymbol{a}_{i+1}^\dagger - \boldsymbol{a}_{i+1}) + \\ &C_-\omega_-\phi_* \sqrt{\frac{1}{2}\sqrt{\frac{L_+}{C_+}}}\left(\boldsymbol{\sigma}_i^y(\boldsymbol{a}_{i+1}^\dagger - \boldsymbol{a}_{i+1}) + (\boldsymbol{a}_i^\dagger - \boldsymbol{a}_i)\boldsymbol{\sigma}_{i+1}^y\right)\Bigg] \end{aligned} \tag{67}$$

## 5.1 Capacitive chain in the resonator limit

As a first step, we can study this problem in the limit where the qubit behaves as a resonator. To simplify the notation, starting from eq. (66), we are going to write the terms of the capacitive coupling as shown in the following example: $\frac{C_C}{2C^2}Q_+^i Q_-^{i+1} = q_+ q_-(\boldsymbol{a}_i^\dagger - \boldsymbol{a}_i)(\boldsymbol{b}_{i+1}^\dagger - \boldsymbol{b}_{i+1})$. This allows us to write the Hamiltonian of the chain as:

$$\begin{aligned} H = \sum_{i=0}^{N}\Big[&\omega_- \boldsymbol{b}_i \boldsymbol{b}_i^\dagger + \omega_+ \boldsymbol{a}_i \boldsymbol{a}_i^\dagger + g_\Phi(\boldsymbol{b}_i^\dagger + \boldsymbol{b}_i)(\boldsymbol{a}_i^\dagger + \boldsymbol{a}_i) + \\ &+q_-^2(\boldsymbol{b}_i^\dagger - \boldsymbol{b}_i)(\boldsymbol{b}_{i+1}^\dagger - \boldsymbol{b}_{i+1}) \\ &+q_+^2(\boldsymbol{a}_i^\dagger - \boldsymbol{a}_i)(\boldsymbol{a}_{i+1}^\dagger - \boldsymbol{a}_{i+1}) \\ &+q_- q_+(\boldsymbol{b}_i^\dagger - \boldsymbol{b}_i)(\boldsymbol{a}_{i+1}^\dagger - \boldsymbol{a}_{i+1}) \\ &+q_- q_+(\boldsymbol{a}_i^\dagger - \boldsymbol{a}_i)(\boldsymbol{b}_{i+1}^\dagger - \boldsymbol{b}_{i+1})\Big] \end{aligned} \tag{68}$$

At this point, it is necessary to apply the RWA to proceed with the analysis:

$$\begin{aligned} H = \sum_{i=0}^{N} \Big[ & \omega_- \boldsymbol{b}_i \boldsymbol{b}_i^\dagger + \omega_+ \boldsymbol{a}_i \boldsymbol{a}_i^\dagger + g_\Phi (\boldsymbol{b}_i^\dagger \boldsymbol{a}_i + \boldsymbol{b}_i \boldsymbol{a}_i^\dagger) + \\ & + q_-^2 (\boldsymbol{b}_i^\dagger \boldsymbol{b}_{i+1} + \boldsymbol{b}_i \boldsymbol{b}_{i+1}^\dagger) \\ & + q_+^2 (\boldsymbol{a}_i^\dagger \boldsymbol{a}_{i+1} + \boldsymbol{a}_i \boldsymbol{a}_{i+1}^\dagger) \\ & + q_- q_+ (\boldsymbol{b}_i^\dagger \boldsymbol{a}_{i+1} + \boldsymbol{b}_i \boldsymbol{a}_{i+1}^\dagger) \\ & + q_- q_+ (\boldsymbol{a}_i^\dagger \boldsymbol{b}_{i+1} + \boldsymbol{a}_i \boldsymbol{b}_{i+1}^\dagger) \Big] \end{aligned} \tag{69}$$

Assuming periodic boundary conditions, we can introduce the bosonic operators in momentum space:

$$\boldsymbol{a}_k^\dagger = \frac{1}{\sqrt{N}} \sum_{n=1}^{N} e^{ikn} \boldsymbol{a}_n^\dagger \ , \quad \boldsymbol{b}_k^\dagger = \frac{1}{\sqrt{N}} \sum_{n=1}^{N} e^{ikn} \boldsymbol{b}_n^\dagger, \tag{70}$$

and rewrite the Hamiltonian as:

$$H = \sum_k \begin{pmatrix} \boldsymbol{a}_k^\dagger & \boldsymbol{b}_k^\dagger \end{pmatrix} \begin{bmatrix} \omega_+ + 2q_+^2 \cos(k) & g_\phi + 2q_+ q_- \cos(k) \\ g_\phi + 2q_- q_+ \cos(k) & \omega_- + 2q_-^2 \cos(k) \end{bmatrix} \begin{pmatrix} \boldsymbol{a}_k^\dagger \\ \boldsymbol{b}_k^\dagger \end{pmatrix} \tag{71}$$

# References

[1] Sergey Bravyi, David P DiVincenzo, and Daniel Loss. Schrieffer–wolff transformation for quantum many-body systems. *Annals of physics*, 326(10):2793, 2011.

[2] María Hita-Pérez, Gabriel Jaumà, Manuel Pino, and Juan José García-Ripoll. Ultrastrong capacitive coupling of flux qubits, 2021.